YMTHE, Volume *31*

Supplemental Information

NLRC3 expression in macrophage impairs glycolysis and host immune defense by modulating the NF-κB-NFAT5 complex during septic immunosuppression

Jiqian Xu, Chenggang Gao, Yajun He, Xiangzhi Fang, Deyi Sun, Zhekang Peng, Hairong Xiao, Miaomiao Sun, Pei Zhang, Ting Zhou, Xiaobo Yang, Yuan Yu, Ruiting Li, Xiaojing Zou, Huaqing Shu, Yang Qiu, Xi Zhou, Shiying Yuan, Shanglong Yao, and You Shang

Fig. S1.

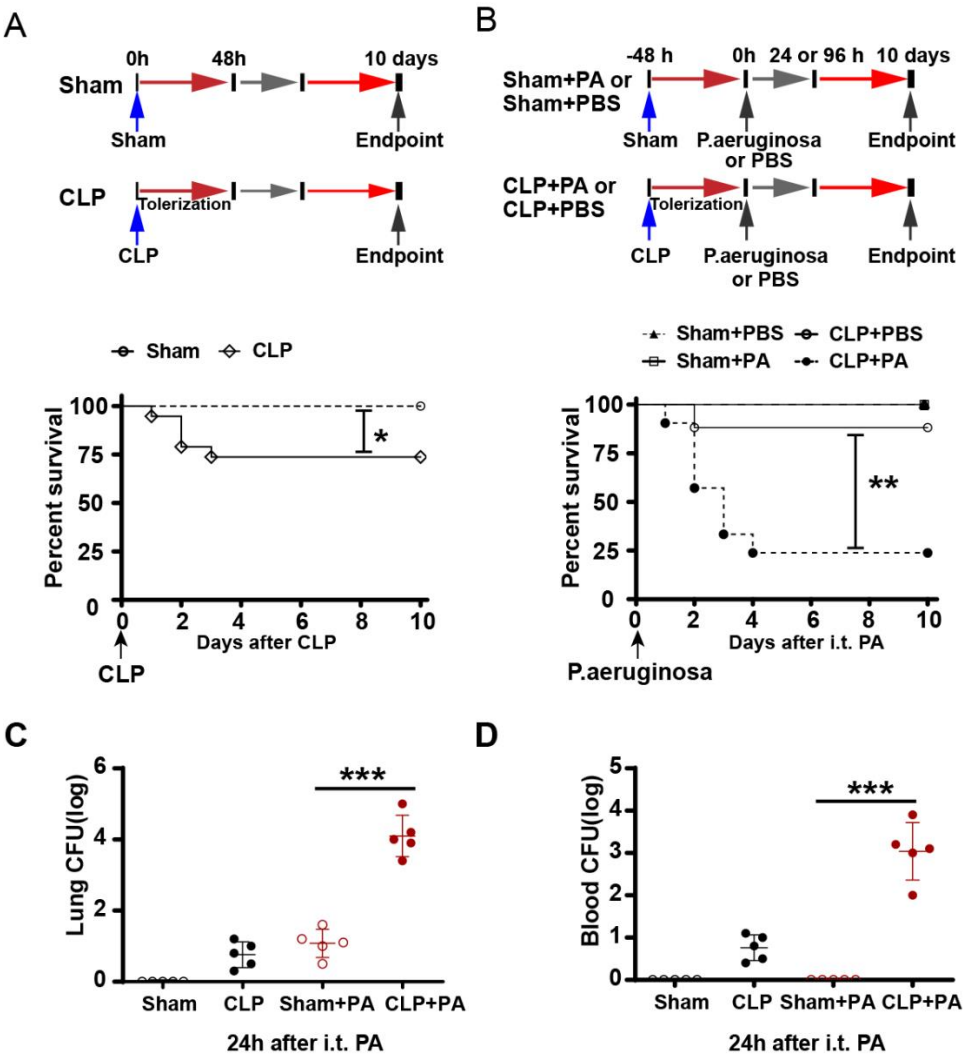

Fig. S1.

Cecal ligation and puncture (CLP) impaired host lung immune responses. Related to Figure 1 and 2. (A-B) Kaplan-Meier survival curves from wild-type (WT) mice subjected to CLP or sham surgery (**A**), surviving CLP or sham mice underwent secondary *P. aeruginosa* infection (n = 19 mice/group) (**B**). *P. aeruginosa* was administered intratracheally 48 h after CLP or sham operation, all mice were monitored for 10 days after operation or *P. aeruginosa* rechallenge for survival (n = 20 mice/group). (**C-D**) Bacterial loads in the lung (**C**) and blood (**D**) of surviving mice were measured 24 h after secondary *P. aeruginosa* infection (n = 6 mice/group). Circles represent individual mice. *P < 0.05; **P < 0.01; ***P < 0.001; NS: not significant (two-way ANOVA or Student's *t* test and log-rank test for survival).

Fig. S2.

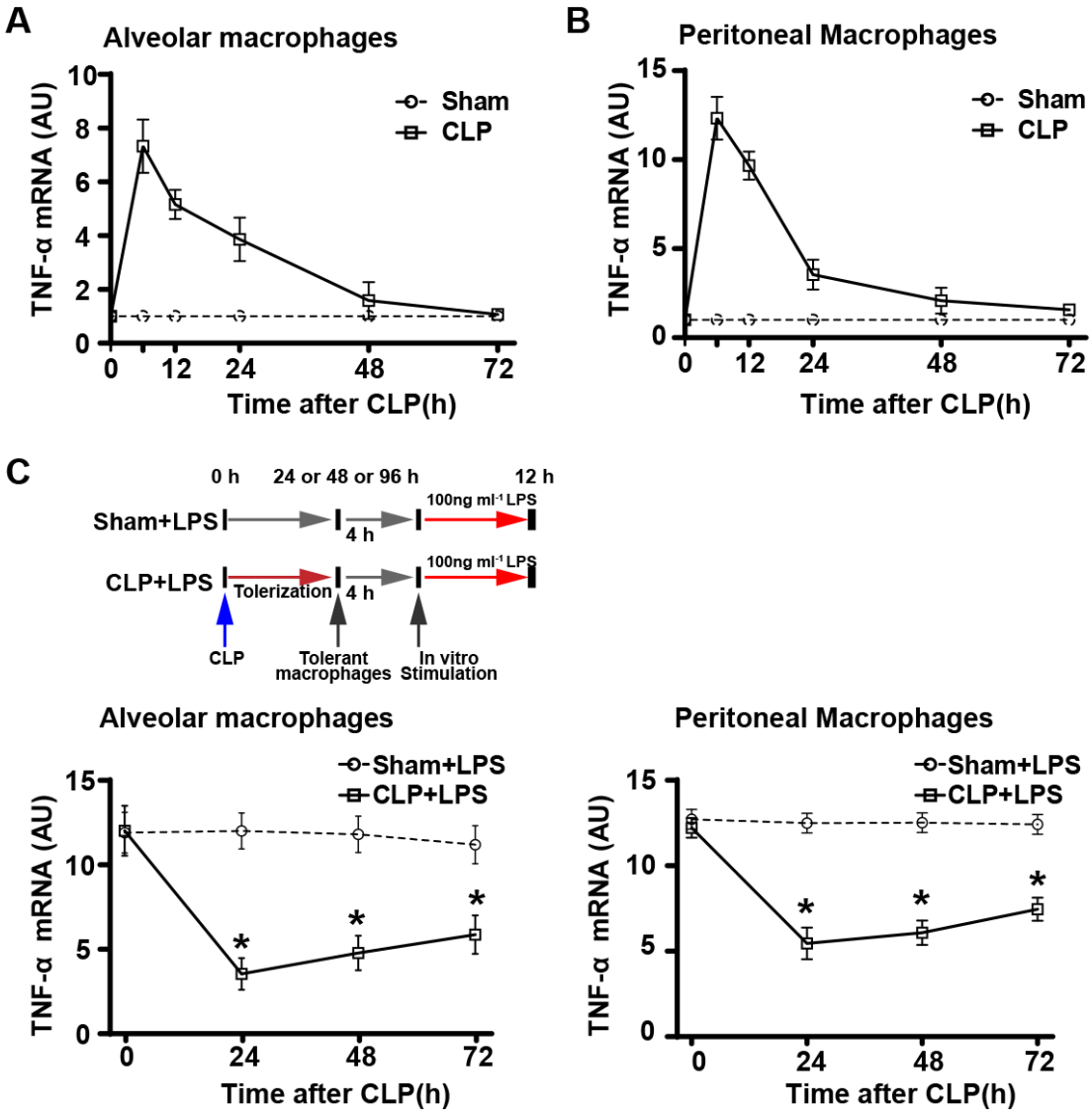

Fig. S2.

CLP impaired immune responses of macrophages. Related to Figure 1 and 2. (**A**-**B**) TNF-α mRNA expression in indicated alveolar macrophages (**A**) and peritoneal macrophages (**B**) at 6, 12, 24, 48, 72, 96, and 120 h after CLP (n = 8 mice/group). (**C**) TNF-α mRNA expression in indicated alveolar macrophages (**left**) and peritoneal macrophages (**right**) with secondary LPS stimulation at 24, 48, and 72 h post CLP or sham operation. (n = 6 mice/group). The data shown are presented as means ± SE, *P < 0.05; (two-way ANOVA or Student's *t* test).

Fig. S3.

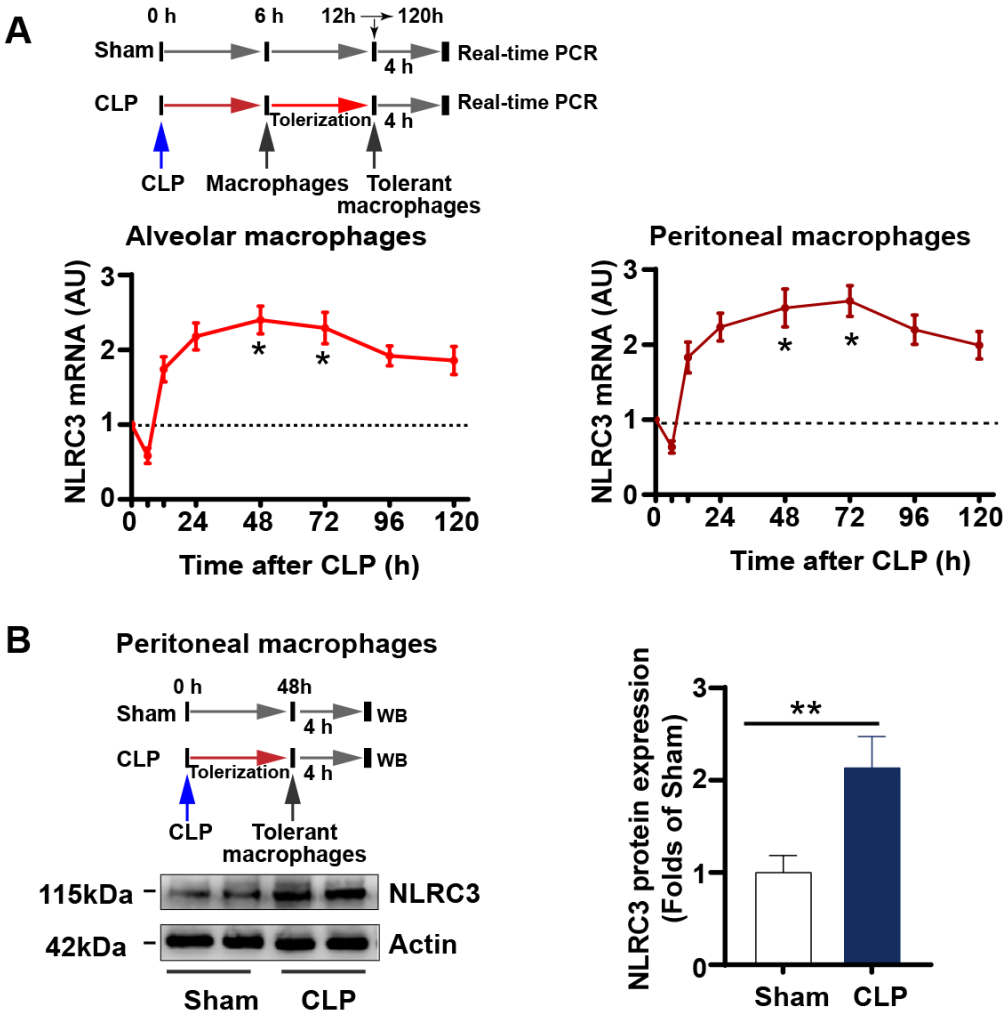

Fig. S3.

CLP induced NLRC3 expression in macrophages. Related to Figure 1 and 2. (**A**) NLRC3 mRNA expression in indicated alveolar macrophages (**left**) and peritoneal macrophages **(right**) at 6, 12, 24, 48, 72, 96, and 120 h after CLP (n = 6 mice/group). NLRC3 protein expression in peritoneal macrophages (**B**) at 48h after CLP operation. The data shown are presented as means ± SE, *P < 0.05; **P< 0.01 (two-way ANOVA or Student's *t* test).

Fig. S4.

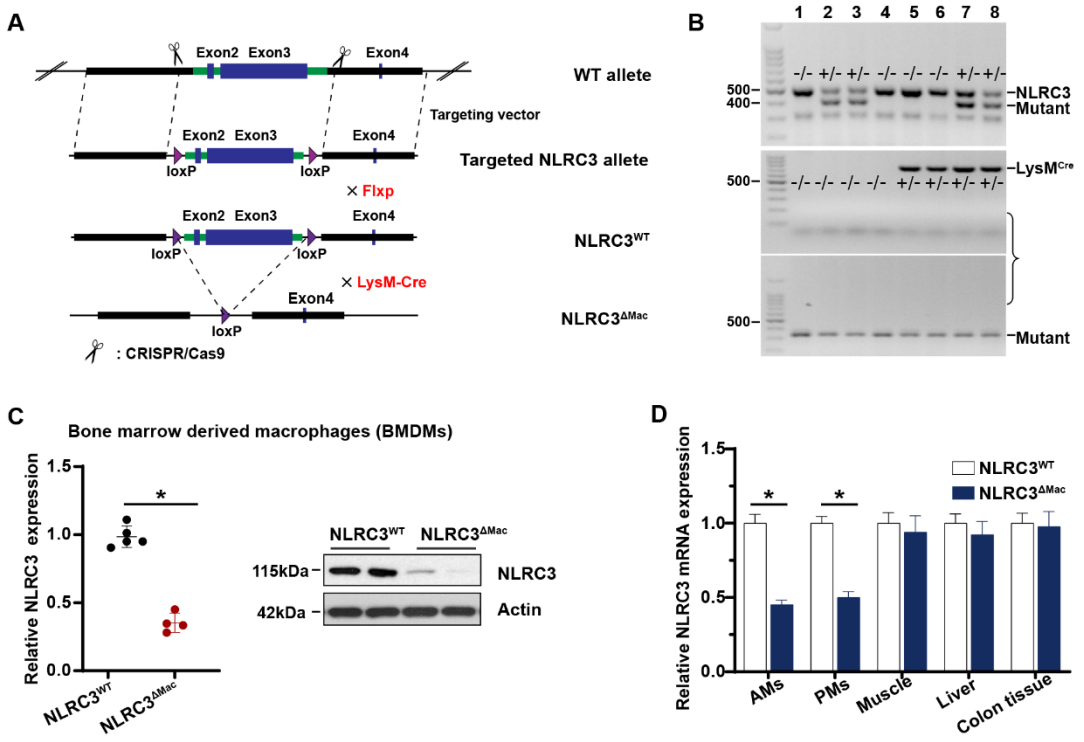

Fig. S4.

Generation of myeloid lineage-specific conditional NLRC3-null mice. Related to Figure 1 and 2. (**A**) A schematic of myeloid lineage-specific conditional NLRC3-null mice generation. Exon 2 was floxed in the targeted allele and excised in the conditional knockout allele. (**B**) Targeted disruption of the *Nlrc3* or *LysM*^{cre} gene was verified by PCR of genomic DNA isolated from candidate mice. (**C**) Immunoblot to detect the NLRC3 expression in BMDMs from NLRC3^{WT} (LysM-Cre-NLRC3$^{fl/fl}$) and NLRC3$^{\Delta Mac}$ (LysM-Cre^{+} NLRC3$^{fl/fl}$). (**D**) Real-time PCR to detect NLRC3 mRNA expression in alveolar macrophages (AMs); peritoneal macrophages (PMs); and muscle, liver, and colon tissue from NLRC3^{WT} and NLRC3$^{\Delta Mac}$ mice. (n = 6 mice/group). Graphs show the mean ± SE of experiment replicates and are representative of at least three independent experiments. *P < 0.05 (one- or two-way ANOVA or Student's *t* test).

Fig. S5.

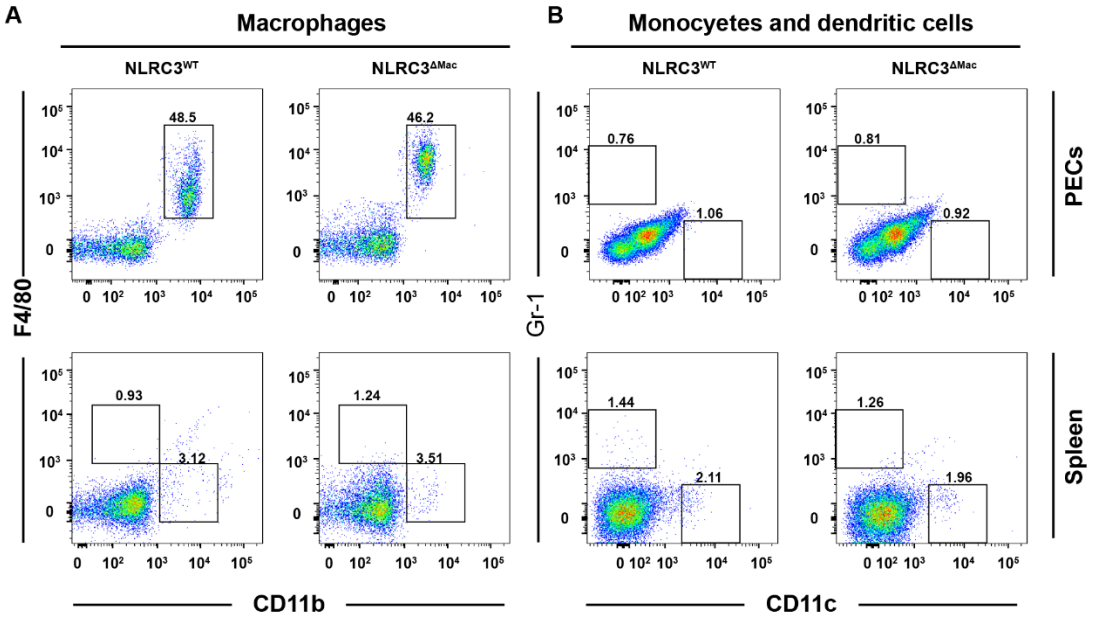

Fig. S5.

Validation of myeloid lineage-specific conditional NLRC3-null mice. Related to Figure 2. (**A-B**) Flow-cytometry analysis of specific cell surface markers for macrophages (**A**) and monocytes (**B**) from the peritoneal cavity (PECs) and spleen tissue isolated from mice of indicated genotypes. NLRC3^{WT} (LysM-Cre-NLRC3$^{fl/fl}$) littermates served as controls for NLRC3$^{\Delta Mac}$ (LysM-Cre^{+} NLRC3$^{fl/fl}$) mice. (n = 6 mice/group). Data are representative of three mice per group from three independent experiments.

Fig. S6.

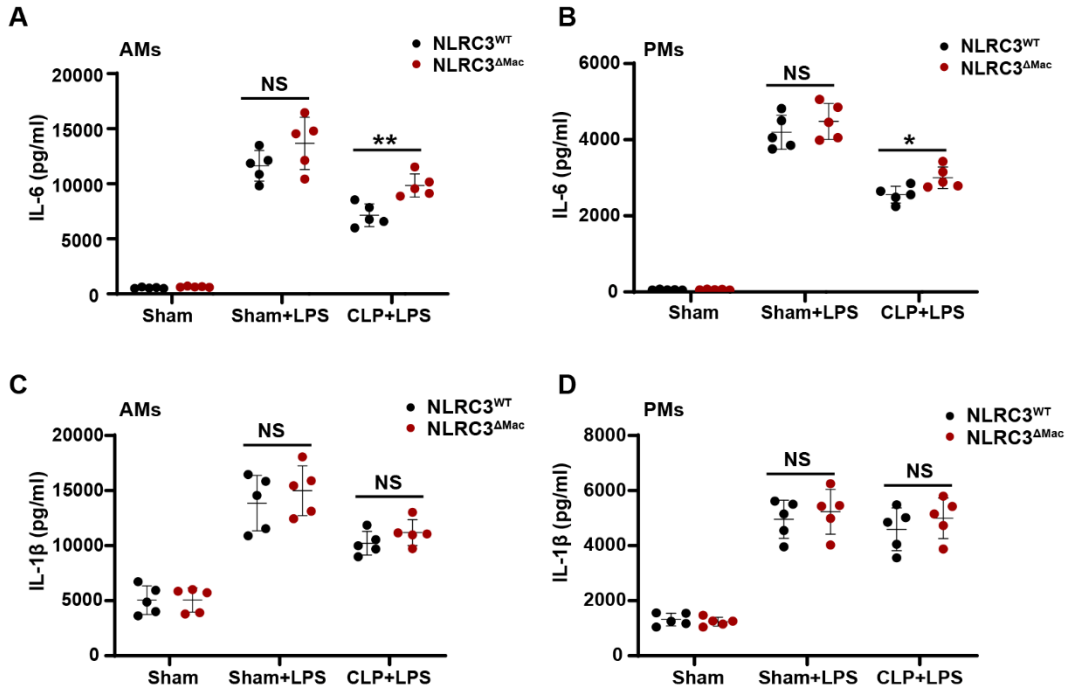

Fig. S6.

NLRC3 depletion improved immune responses of macrophages from septic mice that underwent sepsis-induced immunosuppression. Related to Figure 1. (**A-B**) ELISA for IL-6 in the supernatants of NLRC3^{WT} or NLRC3$^{\Delta Mac}$ mouse AMs (**A**) and PMs (**B**) restimulated with LPS for 12 h at 48 h after CLP or sham operation. (**C-D**) ELISA for IL-1β in the supernatants of NLRC3^{WT} or NLRC3$^{\Delta Mac}$ mouse AMs (**C**) and PMs (**D**) restimulated with LPS for 12 h at 48 h after CLP or sham operation. (n = 5 mice/group). Circles represent individual mice. Graphs show the mean ± SE of experiment replicates; *P < 0.05; NS: not significant (one- or two-way ANOVA or Student's *t* test).

Fig. S7.

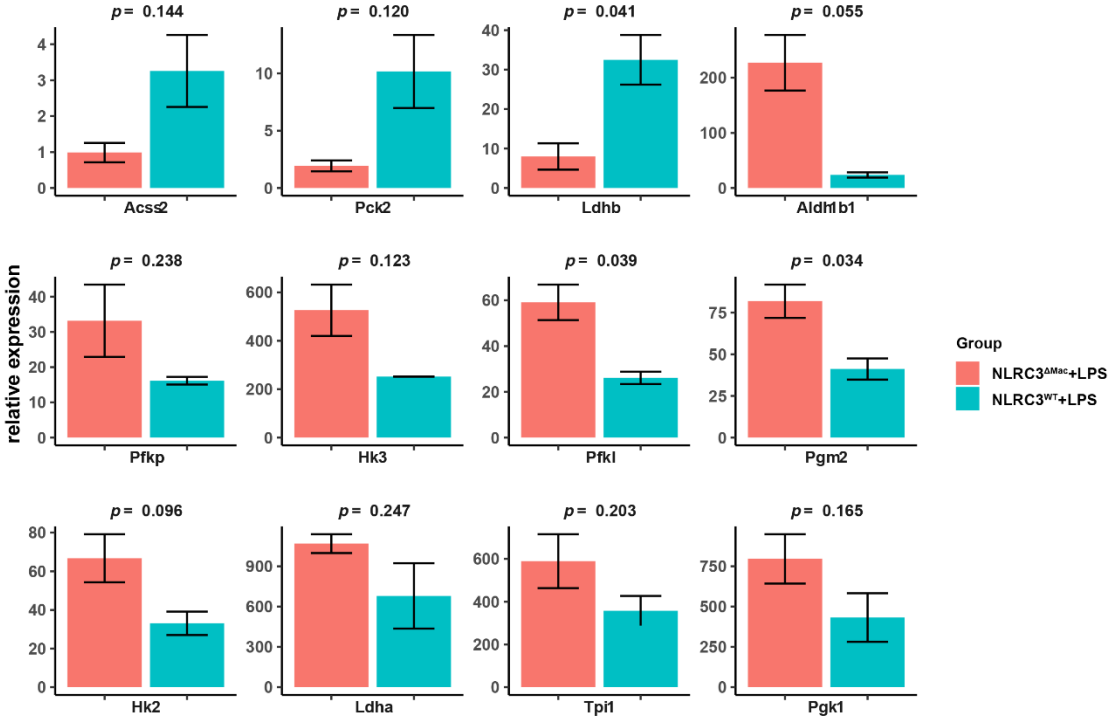

Fig. S7.

Barplots the gene expression in BMDMs from the indicated genotypes. Mouse BMDMs of NLRC3^{WT} (LysM-Cre-NLRC3$^{fl/fl}$) (n=3) and NLRC3$^{\Delta Mac}$ (LysM-Cre^{+} NLRC3$^{fl/fl}$) (n=3) were treated with LPS (100 ng/mL) and then analysed by RNA-seq in 3 pairs of samples. Total RNA of each sample was isolated from 1.0×10^6 BMDMs. Barplots depicting comparison of relative gene expression of several glycolytic genes of interest between NLRC3^{WT} group and NLRC3$^{\Delta Mac}$ group. Depicting p values are from Student's t-test. All tests were two-sided.

Fig. S8.

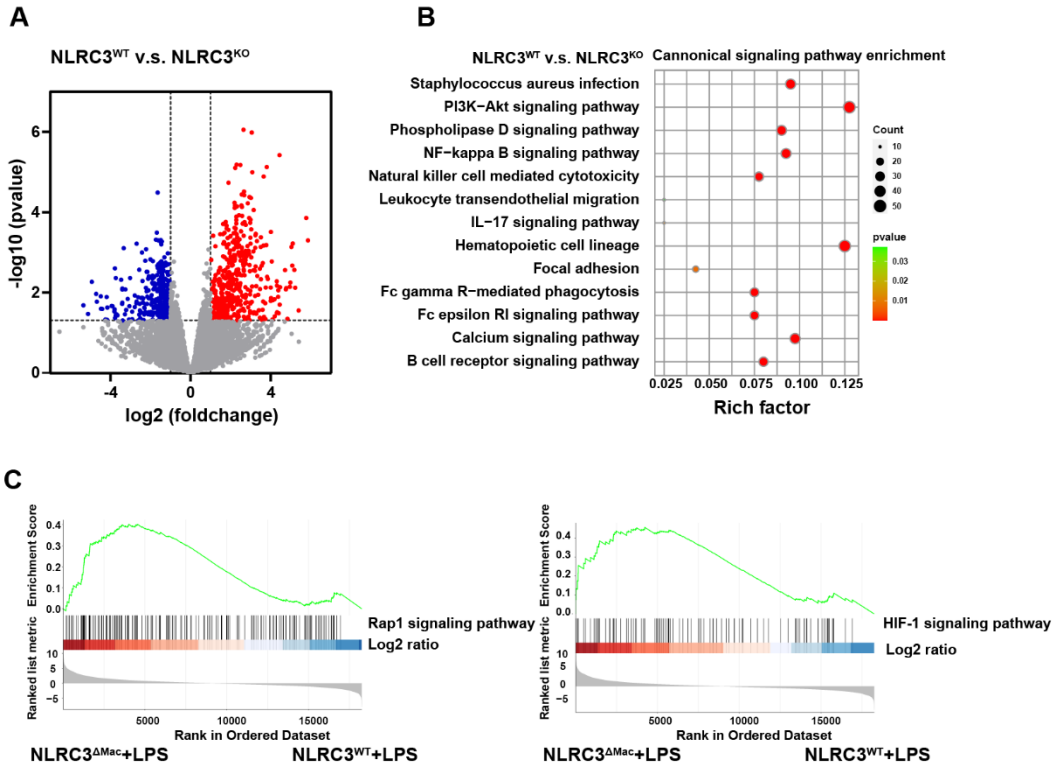

Fig. S8.

Gene expression analysis in BMDMs from the indicated genotypes. (**A**) Volcano plot representation of gene expression (log2 values) alterations of RNA for NLRC3^{WT} (LysM-Cre-NLRC3$^{fl/fl}$) and NLRC3$^{\Delta Mac}$ (LysM-Cre^{+} NLRC3$^{fl/fl}$) macrophages. Red denotes over-expressed genes (log2 fold change ≥1); blue denotes under-expression (log2 fold change ≤-1). The horizontal line depicts multiple comparison adjusted P = 0.05. (**B**) Scatter plot of the KEGG pathway enrichment analysis of the DEGs in immunometabolism-associated pathways between NLRC3^{WT} and NLRC3$^{\Delta Mac}$ macrophages. The Rich factor is the ratio of DEG numbers annotated in this pathway term to all genes. Coloring of the p-values indicates the significance of the Rich factor ranging from −1 to 1. The 13 common pathway terms of three comparisons enriched in the KEGG database are listed in this figure. The size of the symbols represents the number count of DEGs. (**C**) Hallmark gene sets of the above datasets showed that the NLRC3-mediated Warburg effect was closely related to mTOR signaling pathways. NES, normalized enrichment score.

Fig. S9.

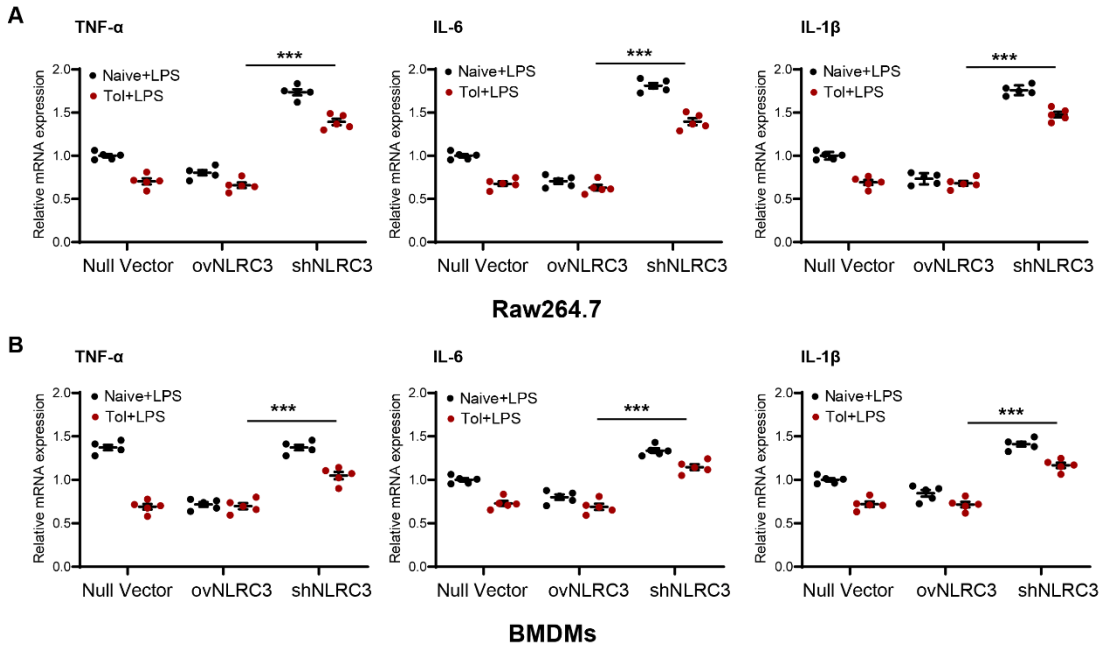

Fig. S9. The *in vitro* tolerance model that imitates sepsis-induced immunosuppression. qPCR detection of TNF-α, IL-6, and IL-1β mRNA expression in tolerant or naïve RAW 264.7 (A)and BMDM (B) macrophages transduced with null, shNLRC3, or ovNLRC3 vector after 12-h LPS restimulation (100 ng/mL) (n = 5). The results of mRNA expression were normalized to β-actin. Graphs show the mean ± SE of experiment replicates and are representative of five independent experiments; (two-way ANOVA or Student's *t* test)

Fig. S10.

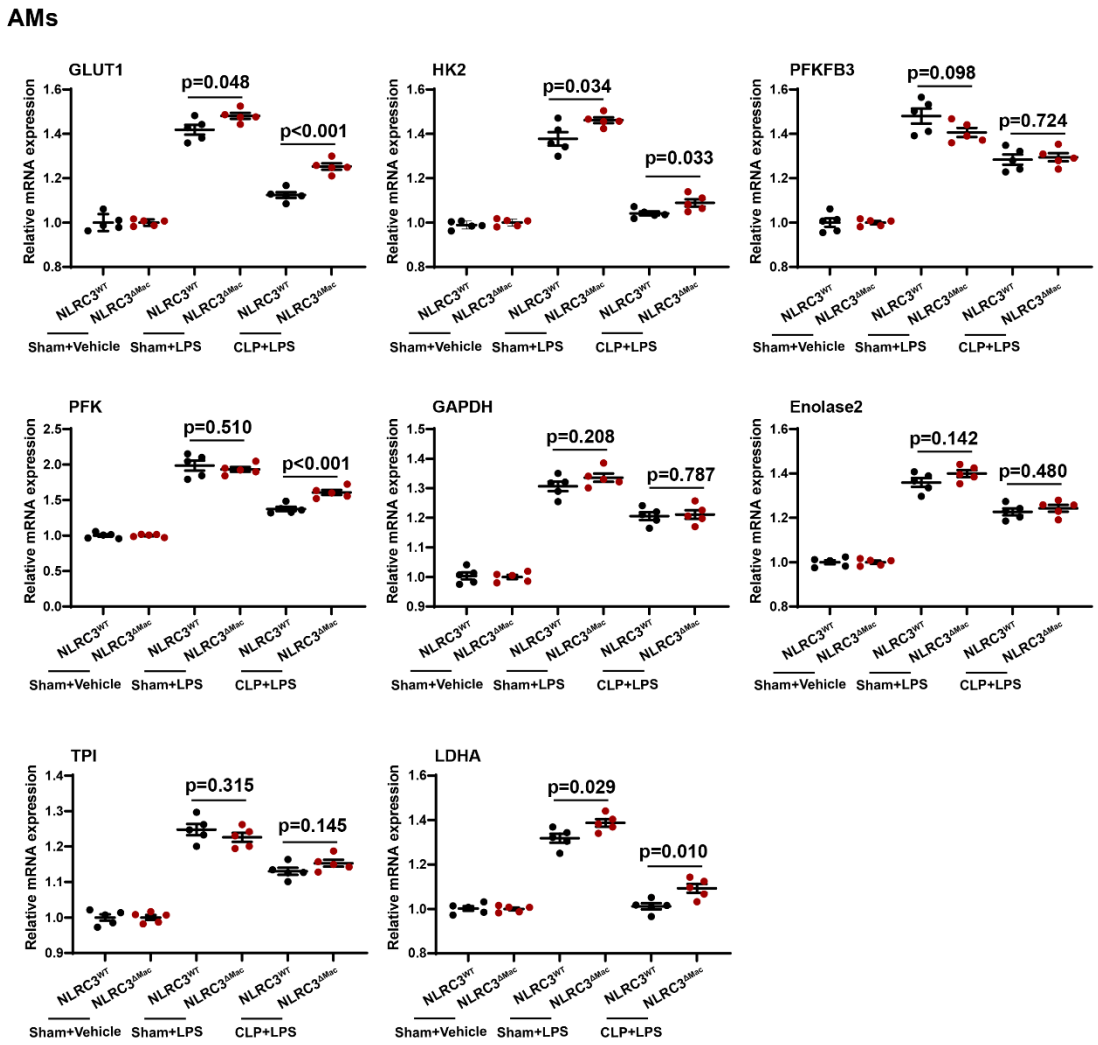

Fig. S10. Glycolytic gene expression within the macrophage from the indicated genotypes. Mouse AMs of NLRC3^{WT} (LysM-Cre-NLRC3$^{fl/fl}$) (n = 5) and NLRC3$^{\Delta Mac}$ (LysM-Cre^{+} NLRC3$^{fl/fl}$) (n = 5) with LPS *in vitro* challenge for 12 h at 48 h after CLP or sham operation (n = 5 mice /each group), qPCR detection of the mRNA expression levels of representative NLRC3-regulated glycolytic gene in macrophages. Circles represent individual mice. Graphs show the mean ± SE of experiment replicates and are representative of five independent experiments; (two-way ANOVA or Student's *t* test).

Fig. S11.

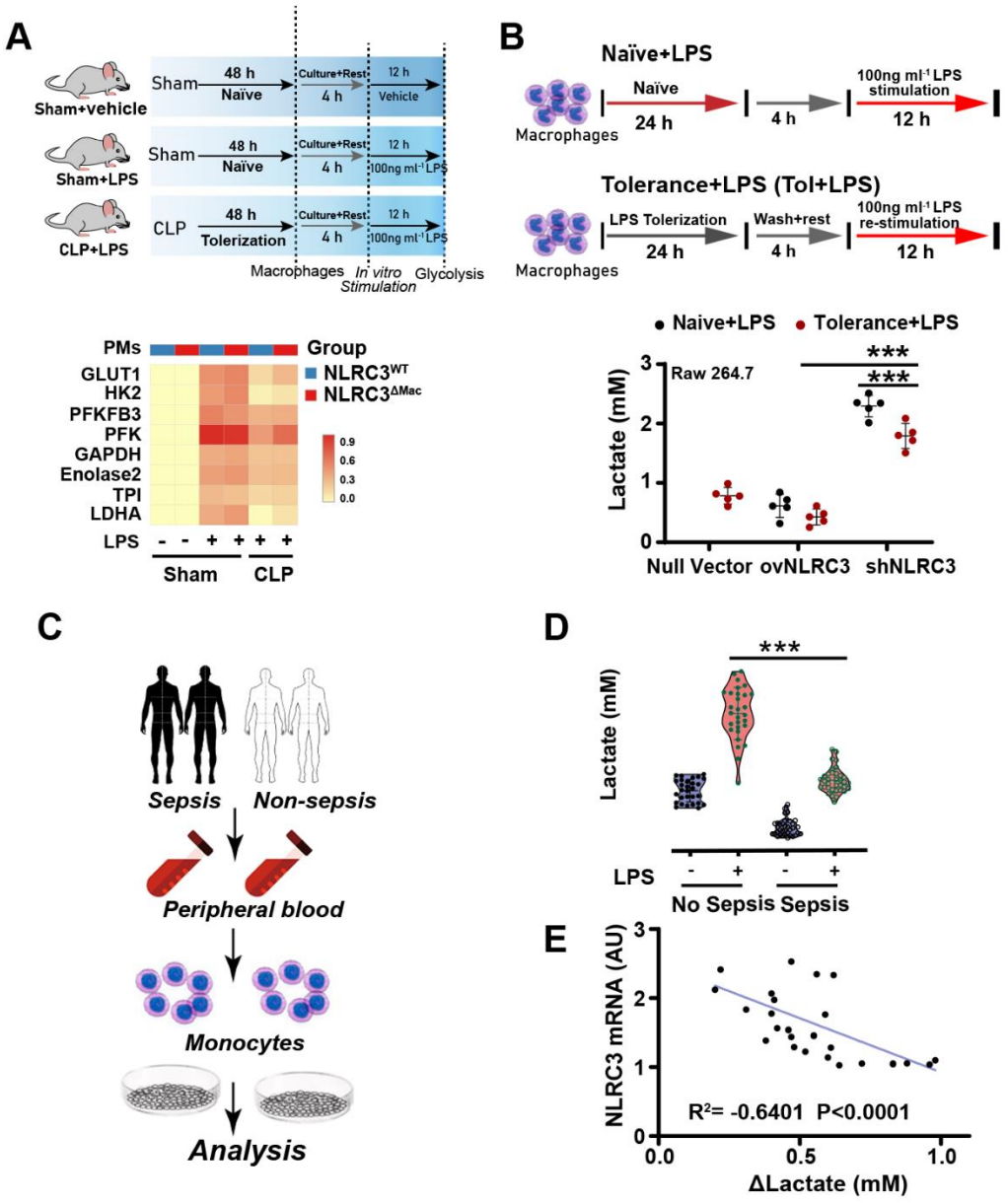

Fig. S11.

Lactate levels in the macrophages of septic mice, and in the monocytes of septic patients and their correlation with NLRC3 mRNA expression. (**A**) qPCR detection of the mRNA expression levels of representative NLRC3-regulated genes involved in glycolysis in PMs. PMs with secondary LPS *in vitro* challenge for 12 h at 48 h after CLP or sham operation (n = 5). The results of mRNA expression were normalized to β-actin, and log2 values were used to calculate correlations. Each column in the heat map represents the ratio of normalized expression (n = 5). (**B**) RAW 264.7 with null vector, stable NLRC3 deficiency (shNLRC3), or overexpression (ovNLRC3) were tolerized with 100 ng/mL LPS (tolerant) or left untreated (naïve) for 24 h, these cells

washed with PBS, cultured in medium (2 h), and stimulated with 100 ng/mL LPS for 12 h. ELISA for lactate production. (**C**) Schematic overview of experimental design for **(D–E)**. (**D**) ELISA for Lactate in the culture supernatants of sepsis patient (n = 21) and non-sepsis donor monocyte (n = 15) stimulated with or without LPS *in vitro* (10 ng/mL) for 12 h (data are presented in a violin plot, *t* test). (**E**) Correlation assay between NLRC3 and change in lactate production (Δlactate: RPMI-stimulated monocytes versus LPS-stimulated monocytes) in monocytes and from indicated sepsis patients (n = 21). Circles represent individual values. Graphs show the mean ± SE of experiment replicates and are representative of at least three independent experiments; ***P < 0.001(two-way ANOVA or Student's *t* test).

Fig. S12.

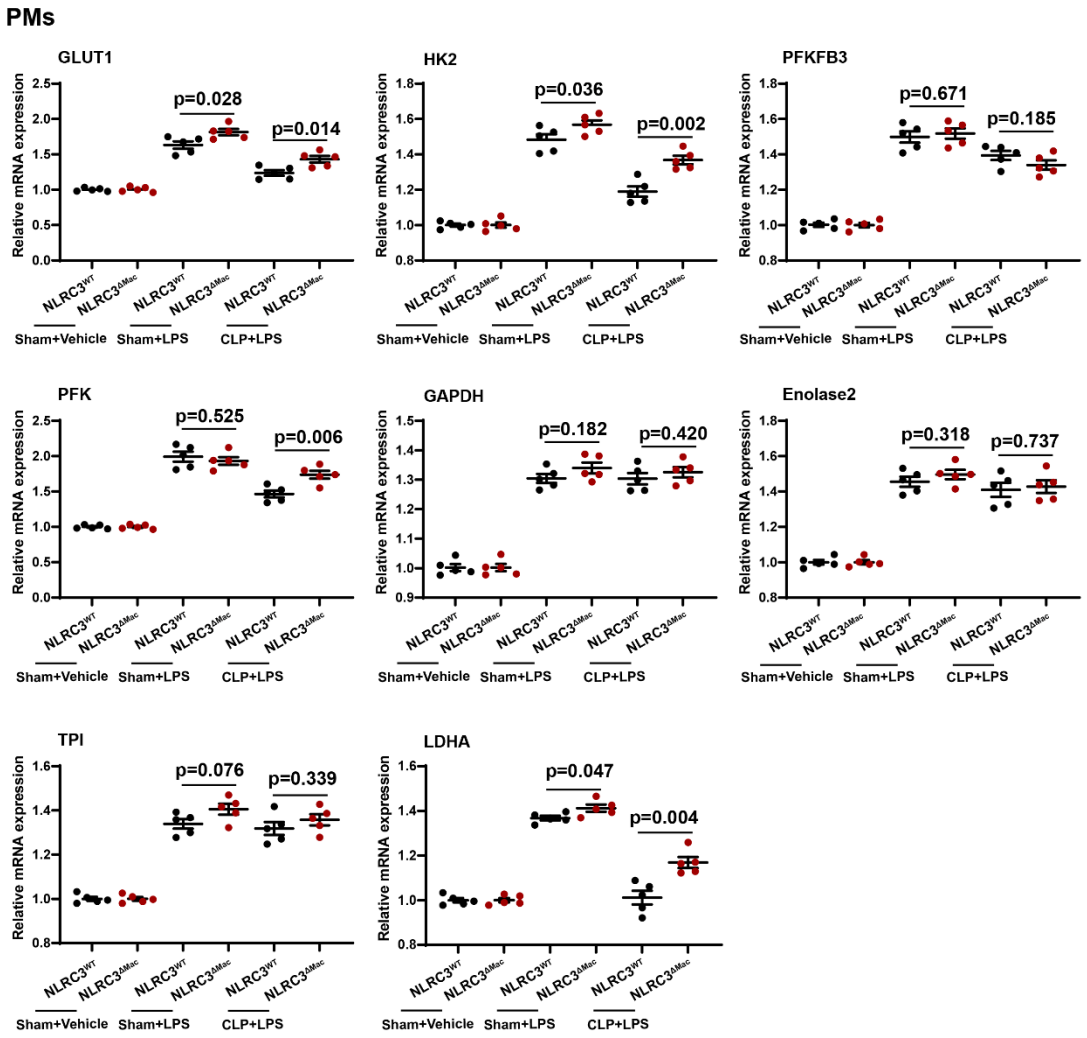

Fig. S12. Glycolytic gene expression within the macrophage from the indicated genotypes. Mouse PMs of NLRC3^{WT} (LysM-Cre-NLRC3$^{fl/fl}$) (n = 5) and NLRC3$^{\Delta Mac}$ (LysM-Cre^{+} NLRC3$^{fl/fl}$) (n = 5) with LPS *in vitro* challenge for 12 h at 48 h after CLP or sham operation (n = 5 mice /each group), qPCR detection of the mRNA expression levels of representative NLRC3-regulated glycolytic gene in macrophages. The results of mRNA expression were normalized to β-actin. Circles represent individual mice. Graphs show the mean ± SE of experiment replicates and are representative of five independent experiments; (two-way ANOVA or Student's *t* test).

Fig. S13.

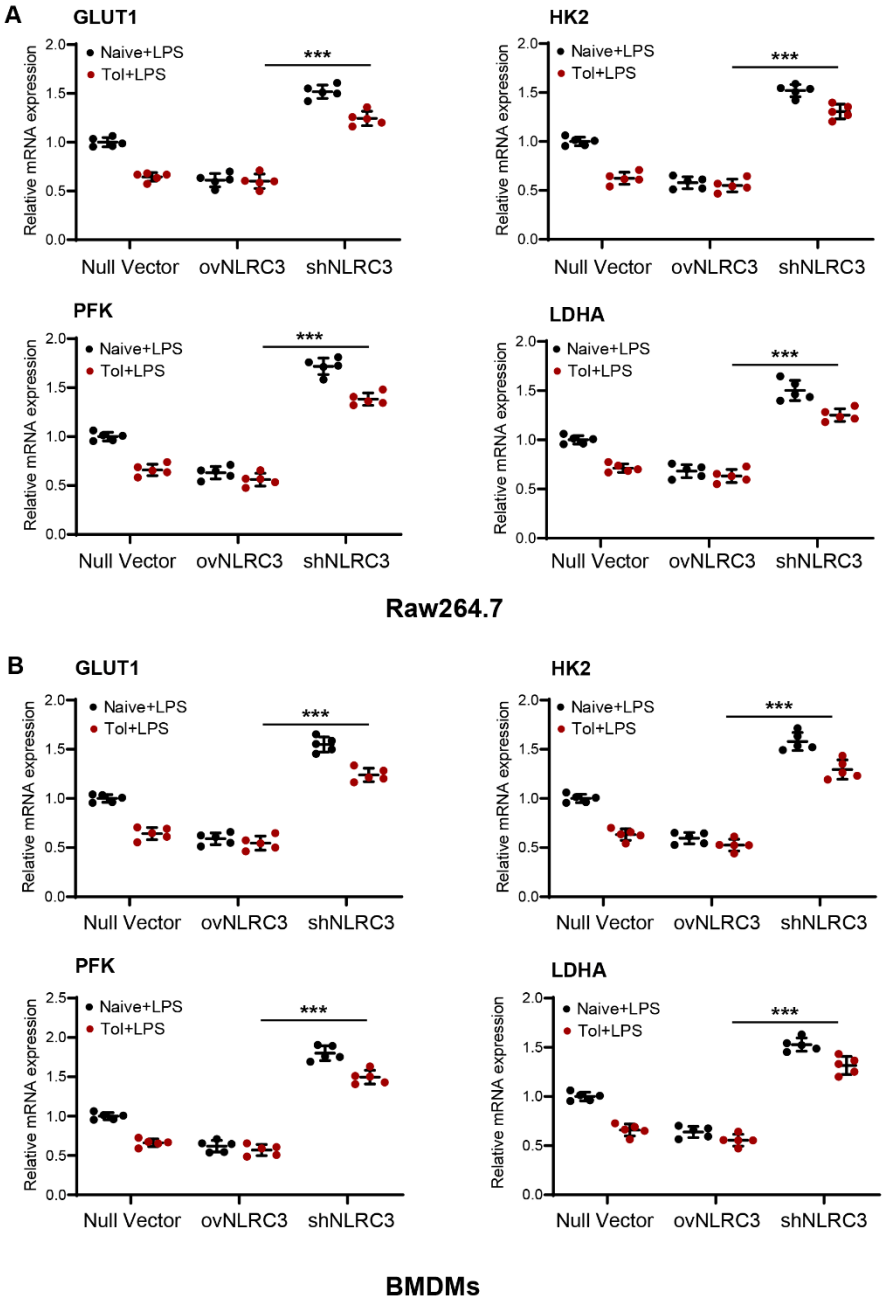

Fig. S13. Glycolytic gene expression within the macrophage from the indicated genotypes. RAW 264.7(A) and BMDMs (B)with null vector, NLRC3 deficiency (shNLRC3), or overexpression (ovNLRC3) were tolerized with 100 ng/mL LPS (tolerant) or left untreated (naïve) for 24 h, these cells washed with PBS, cultured in medium (2 h), and stimulated with 100 ng/mL LPS for 12 h. The results of mRNA expression were normalized to β-actin, Circles represent individual values. Graphs show the mean ± SE of experiment replicates and are representative of five independent experiments; ***P < 0.001 (two-way ANOVA or Student's *t* test).

Fig. S14.

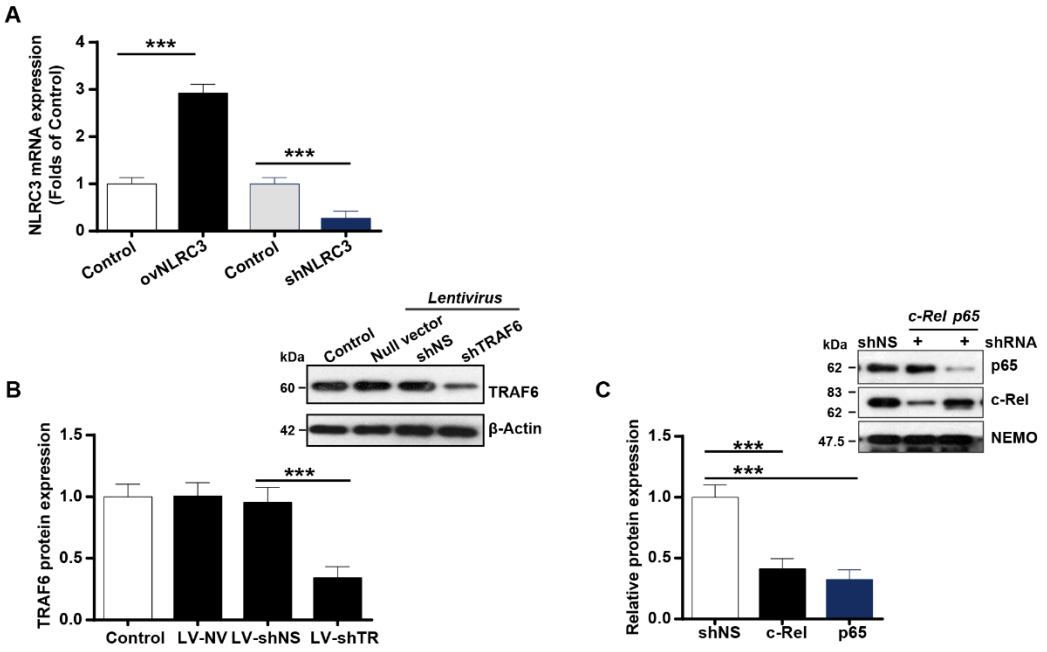

Fig. S14.

RNAi validation in the macrophages. qPCR to detect NLRC3 mRNA expression in RAW 264.7 stably transduced with shNLRC3 or overexpressing NLRC3 (ovNLRC3) (**A**) Immunoblots to detect TRAF6, p65 and c-Rel expression (**B-C**) in RAW 264.7 stably transduced with shNLRC3 after transfection with the indicated vector (shp65, shRel, or shNS). (n = 3). Graphs show the mean ± SE of experiment replicates and are representative of at least three independent experiments; ***P < 0.001; NS, not significant (two-way ANOVA or Student's *t* test).

Fig. S15.

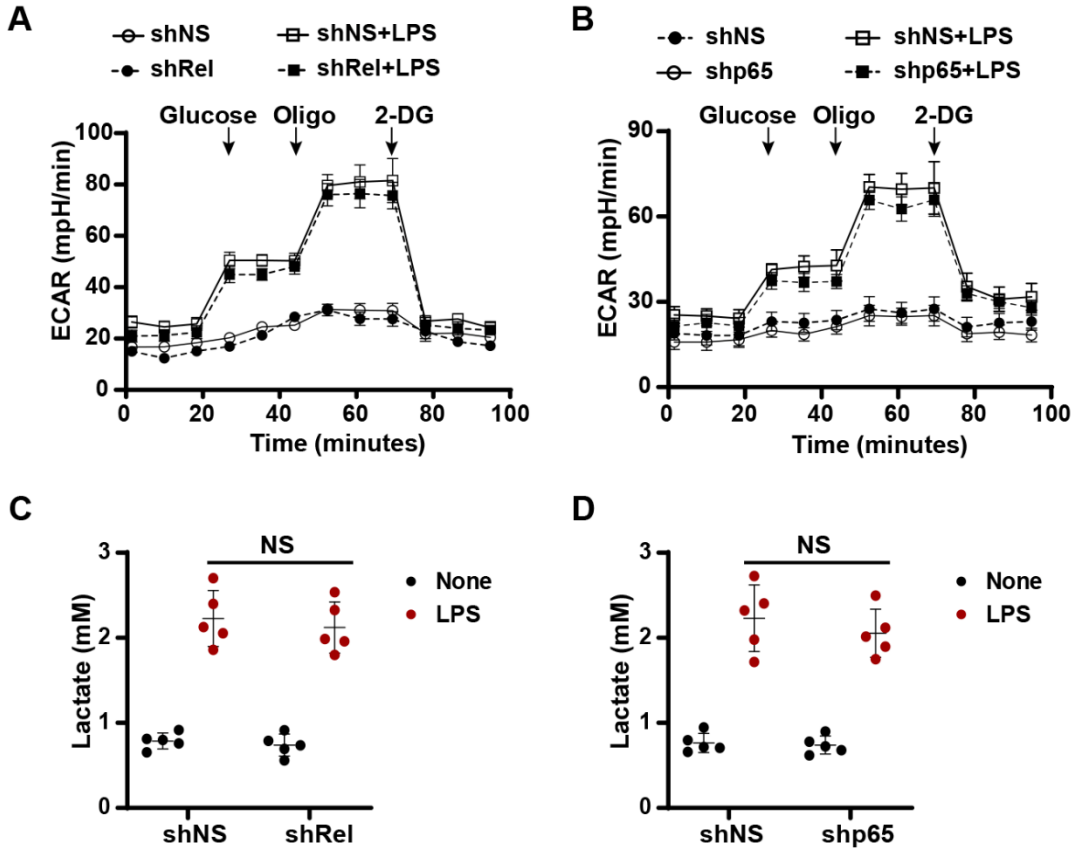

Fig. S15.

NF-κB subunit depletion in macrophages does not alter NLRC3 deficiency-dependent glycolysis or inflammatory responses. RAW 264.7 with stable NLRC3 deficiency were transfected with shp65 or shRel or shNS (control) vector, then cells were tolerized with 100 ng/mL LPS (Tol) or left untreated (Naïve) for 24 h. The tolerant cells were washed with PBS, cultured in medium (2 h), and restimulated with 100 ng/mL LPS for 12 h; the Naïve cells were cultured in medium without LPS for 14 h. (**A, B**) Seahorse XF^e 24 monitored ECAR. (**C, D**) ELISAs for lactate production in tolerant BMDMs of $NLRC3^{\Delta Mac}$ with shp65 or shRel or shNS (control) vector after 12-h LPS restimulation (n = 5), the naïve BMDMs with shp65 or shRel or shNS vector in the absence of LPS stimulation served as the control groups. Circles represent individual values. Graphs show the mean ± SE of experiment replicates and are representative of at least three independent experiments; NS, not significant (two-way ANOVA or Student's *t* test).

Fig. S16.

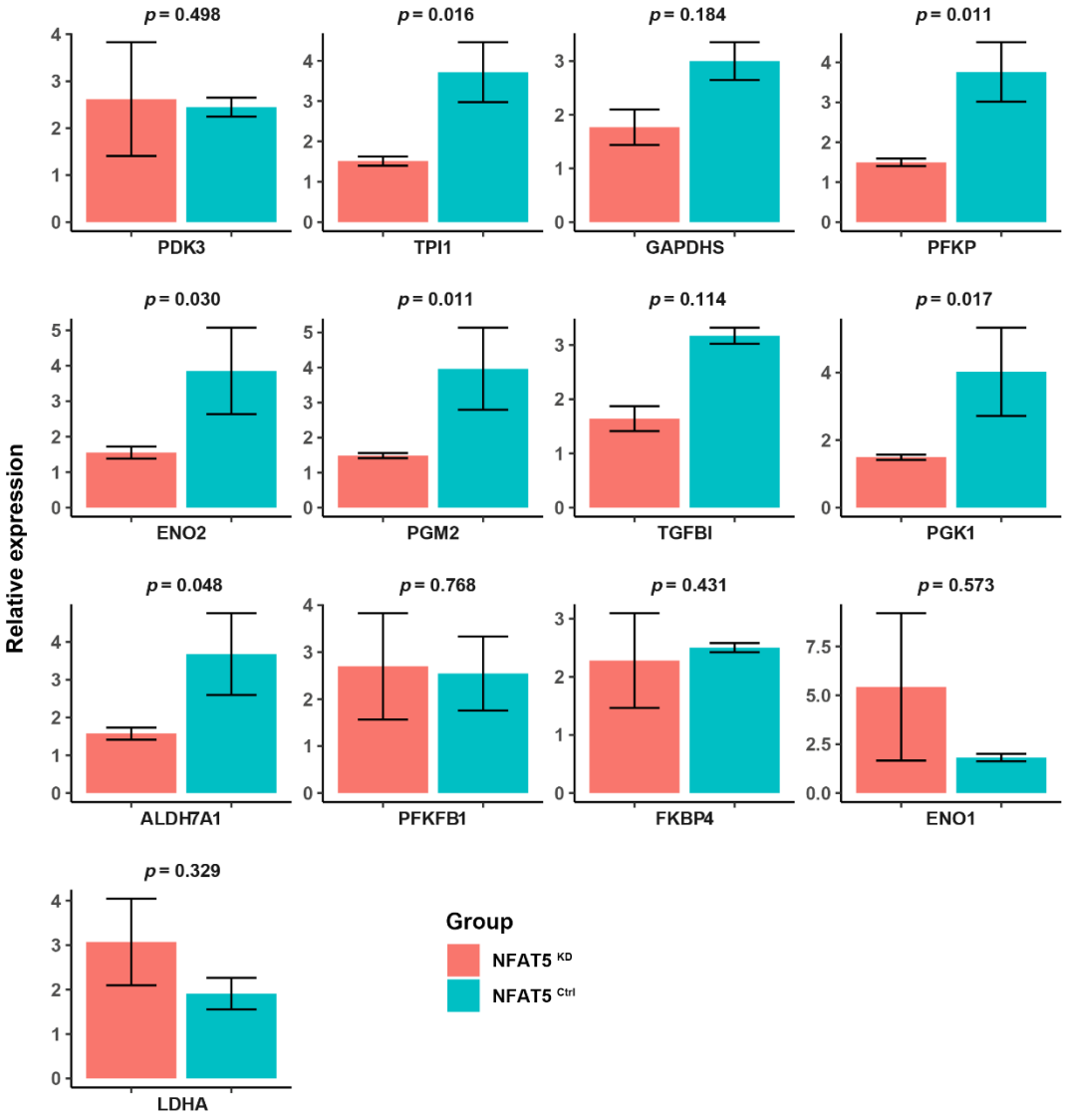

Fig. S16.

Barplots the gene expression in RAW 264.7 with NFAT5 knockdown. RNA-seq data comparing NFAT5 shRNA (NFAT5 ^{KD}) and transduced empty vector (NFAT5^{Ctrl}) RAW 264.**7** from the NCBI GEO database (GSE76554). Barplots depicting comparison of relative gene expression of several glycolytic genes of interest between NFAT5^{KD} macrophages (n = 3) and NFAT5^{Ctrl} macrophages (n = 3). Depicting p values are from Student's t-test. All tests were two-sided.

Fig. S17.

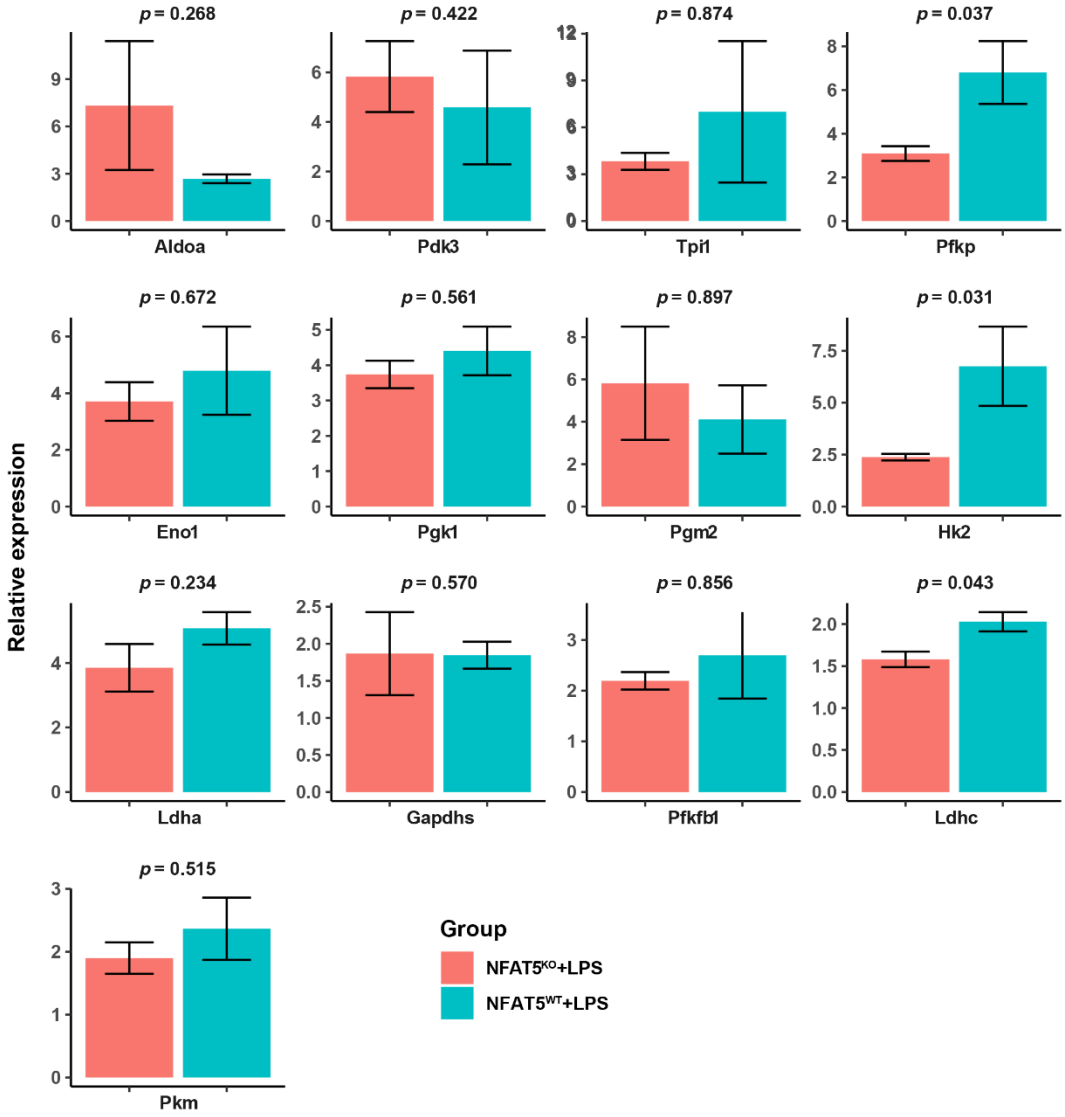

Fig. S17.

Barplots the gene expression in BMDMs with NFAT5 knockout. RNA-seq data comparing NFAT5 KO BMDMs (NFAT5 ^{KO}) and NFAT5 WT BMDMs (NFAT5^{WT}) from the NCBI GEO database (GSE26343). Barplots depicting comparison of relative gene expression of several glycolytic genes of interest between NFAT5^{KO} BMDMs (n = 3) and NFAT5^{WT} BMDMs (n = 3). Depicting p values are from Student's t-test. All tests were two-sided.

Fig. S18.

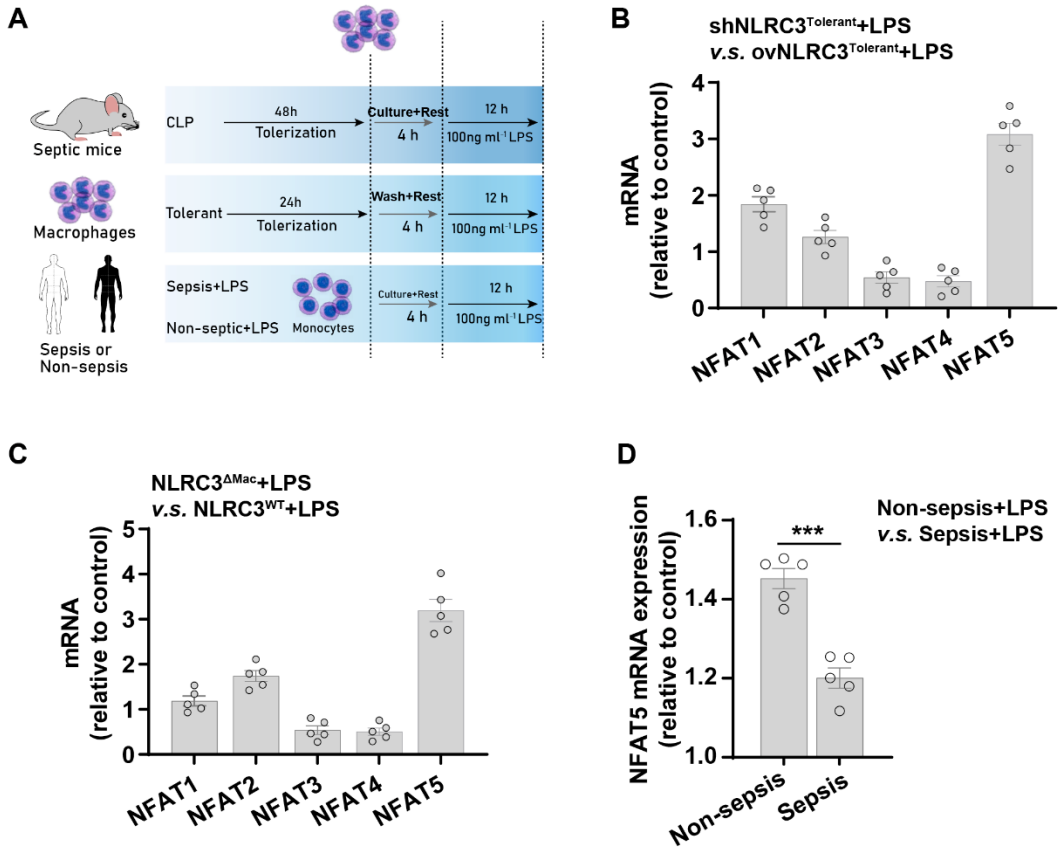

Fig. S18.

(**A**) Schematic overview of experimental design for **(B–D)**. RAW 264.7 with stable NLRC3 deficiency (shNLRC3) or overexpression (ovNLRC3) were tolerized with 100 ng/mL LPS (Tol) or left untreated (naïve) for 24 h, the tolerant cells washed with PBS, cultured in medium (2 h), and restimulated with 100 ng/mL LPS for 12 h, the Naïve cells were cultured for 14 h in medium without LPS. **(B-D)** Real-time PCR to detect the NFAT1-5 mRNA expression (n = 5) in RAW 264.7, in PMs from mice of the indicated genotypes at 48 h after CLP operation (n = 5), and in monocytes from the septic patients or non-septic donors (n = 5) **(D)**. Cells without LPS treatment served as corresponding control group. Circles represent individual values. Graphs show the mean ± SE of experiment replicates and are representative of at least three independent experiments; **P < 0.01; ***P < 0.001; (two-way ANOVA or Student's *t* test).

Fig. S19.

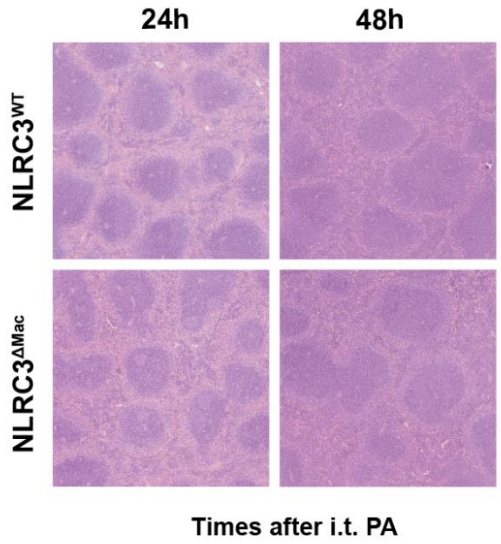

Fig. S19.

NLRC3 depletion in myeloid cells does not aggravate spleen injury in septic mice that underwent sepsis-induced immunosuppression The surviving mice of indicated genotypes ($NLRC3^{WT}$ or $NLRC3^{\Delta Mac}$ mice) underwent secondary *P. aeruginosa* infection. *P. aeruginosa* (1×10^9 CFU) were administered intratracheally 2 days after CLP or sham operation. Histopathological images of spleen tissues. Scale bar represents 50 μm (n = 6 mice/group).

Table S1.

Primers for validation of myeloid lineage-specific conditional NLRC3-null mice. Related to materials and methods.

Primer name	Primer sequence (5’-3’)
L-GT-F1	GATGTACCAACAAAATGCTTAGCTCTC
L-GT-R1	GACGCCTAGATTGTGCTACTCTCAGCT
R-GT-F1	CGTGCTAGATCGACTGCTAGAGTGAC
R-GT-R1	CCATCTCCACACTGATCTCCTCTCC

Table S2.

Human and mouse primers for RT-PCR. Related to materials and methods.

Gene name	Forward primer	Reverse primer
human NLRC3	GTGCCGACCGACTCATCTG	GTCCTGCACTCATCCAAGC
human TNF-α	GGCATTGATGACTCCAGTGTT	ATGGAGCCCAGCAGCAA
human β-actin	TTGAAGGCTGGATTTCCTTTGGGC	TCGTCGCAGATGAAATAGGGCTGT
mouse NLRC3	GTCAGCTGCTACAAGTCCGGGAC	GAGCCTCAGAGTGTTCGGTATCC
mouse TNF-α	CATCTTCTCAAAATTCGAGTGACAA	TGGGAGTAGACAGGTACAACCC
mouse IL-1β	CGGCACACCCACCCTG	AAACCTTTTTCCATCTTCTTCT
mouse IL-6	CTGCAAGAGATTCCATCCAGTT	GAAGTAGGGAAGGCCGTGG
mouse GLUT1	CCCAACTTCTTCAAGATGGTGG	AGAGGCTCAACCATGGTTGC
mouse Hk2	TGATCGCCTGCTTATTCACGG	AACCGCCTAGAAATCTCCAGA
mouse LDHA	CATTGTCAAGACAGTCCACACT	AACCGCCTAGAAATCTCCAGA
mouse PFK1	GGAGGCGAGAACACAAGCC	CGGCCTTCCCTCGTAGTGA
mouse PFKFB3	CCCAGAGCCGGGTACAGAA	GGGGAGTGGTCAGCTTCG
mouse Enolase2	TGCGTCCACTGGCATCTAC	CAGAGCAGGCGCATAGTTTTA
mouse TPI	CCAGGAAGTCTTCGTTGGGG	CAAAGTCGATGTAAGCGGTGG
mouse NFAT1	GACCCGGAGTTCGACTTCG	TGACACTAGGGGACACATAACTG
mouse NFAT2	CTCGGCCTTTGCCCATCTC	AGGAGCACGGAGCATCTGA
mouse NFAT3	TGCTCAACTTCCGTCAAGGAC	GATGTGGTAAGCCAAGGGATG
mouse NFAT4	GAGCTGGAATTTAAGCTGGTGT	CATGGAGGGGTATCCTCTGAG
mouse NFAT5	TGCTTTCTCAGCTTACCACGG	GTCCGCACAACATAGGGCTC
mouse β-actin	CCGTAAAGACCTCTATGCCAACAC	CCACACAGAGTACTTGCGCTCA

Table S3.

Demographic and clinical characteristics of the septic patients, Related to Figure 1

	All patients (n = 64)	**Sepsis (n = 35)**	**Non-Sepsis (n = 29)**
Age, years, mean (±SD)	64.0±14.9	64.0±13.5	64.1±16.7
Male	39 (60.9)	19 (54.3)	20 (69.0)
SOFA	8 [6- 9]	8 [7 - 9]	6 [5 - 8]
Time from sepsis onset to ICU admission, days	-	9 [7–12]	-
Source of Infection			
Abdominal	26 (40.6)	26 (74.3)	0 (0.0)
Pulmonary	19 (29.7)	19(54.3)	0 (0.0)
Urinary	6 (9.4)	6 (17.1)	0 (0.0)
Soft tissue	3 (4.7)	3 (8.6)	0 (0.0)
Others	7 (10.9)	7 (20.0)	0 (0.0)
Microbiology laboratory			
Gram-negative bacteria	32 (50.0)	32 (91.4)	0 (0.0)
Gram-positive bacteria	9 (14.1)	9 (25.7)	0 (0.0)
Others	4 (11.1)	4 (19.1)	0 (0.0)
Secondary pulmonary infection	19 (29.7)	19 (54.3)	0 (0.0)
Chronic comorbidity			
Diabetes	6 (9.4)	4 (11.4)	2 (6.9)
Cardiovascular insufficiency	10 (15.6)	5 (14.3)	5 (17.2)
Respiratory insufficiency	5 (7.8)	2 (5.7)	3 (10.3)
Others	22 (34.4)	12 (34.3)	10 (34.5)
Interventions in ICU			
Central venous catheter	49 (76.6)	30 (85.7)	19 (65.5)
Surgical drain	38 (59.4)	24 (68.6)	14 (48.3)
Mechanical ventilation	62 (96.9)	35 (100.0)	27 (93.1)
Renal replacement therapy	17 (26.6)	13 (37.1)	4 (13.8)
Outcome			
Hospital stay, median (IQR), d	16.5 [11 –24]	20 [10 – 27]	15 [12 – 21]
ICU stay, median (IQR), d	8 [3 –14.0]	14 [9 – 23]	5 [2 – 6]
28-day mortality, n (%)	14 (21.9)	14 (40.0)	0 (0.0)

Abbreviations: ICU, intensive care unit; IQR, interquartile range; SOFA, sequential organ failure assessment; SD, standard deviation;
Data were expressed as count (%) unless otherwise.

Table S4. key reagent

REAGENT	SOURCE	IDENTIFIER
TruStain fcX (anti-mouse CD16/32)	Biolegend	Cat#101320
Anti-mouse CD11b, FITC, Clone M1/70	BD Biosciences	Cat#561688
Anti-mouse F4/80, BV421, Clone T45-2342	BD Biosciences	Cat#565411
Anti-mouse CD11c, BB700, Clone HL3	BD Biosciences	Cat#566505
Anti-mouse Ly-6G Ly-6C, BV605, Clone RB6-8C5	BD Biosciences	Cat#563299
Anti-mouse CD86, PE-Cy7, Clone GL1	BD Biosciences	Cat#560582
Anti-mouse CD206, Alexa 647, Clone MR5D3	BD Biosciences	Cat#565250
Anti-mouse I-A I-E, PE, Clone M5/114.15.2	BD Biosciences	Cat#562010
Anti-human anti-CD14, Alexa 700, clone63D3	BioLegend	Cat#367114
Anti-human anti-HLA-DR, Alexa 488, cloneL243	BioLegend	Cat#307619
Mouse HLA-DR, PE, Clone TU36	BD Biosciences	Cat#555561
Mouse CD14, FITC, Clone M5E2	BD Biosciences	Cat#555397
Anti-NLRC3	Abcam	Cat#ab77817
Anti-p65 (S536), clone: 93H1	Cell Signaling Technology	Cat#3033
Anti-NFAT, clone: D43B1	Cell Signaling Technology	Cat#5861
Anti-NFAT5	Abcam	Cat# ab3446
Anti-p mTOR (Ser2448), clone: D9C2	Cell Signaling Technology	Cat#5536
Anti-p4E-BP1 (Thr37/46), clone: 236B4	Cell Signaling Technology	Cat#2855
Anti-pS6K (Thr389)	Cell Signaling Technology	Cat#9205
Anti-TRAF6, Clone: D-10	Santa Cruz Biotechnology	Cat# sc-8409
Anti-K63 Ub, Clone: D7A11	Cell Signaling Technology	Cat# 5621S
HRP-linked anti-mouse IgG secondary antibody	Cell Signaling Technology	Cat#7076
HRP-linked anti-rabbit IgG secondary antibody	Cell Signaling Technology	Cat#7074
Fixation Buffer	Biolegend	Cat#420801
Intracellular Permeabilization Wash Buffer	Biolegend	Cat#421002
Collagenase IV	Sigma	Cat#C5138
Deoxyribonuclease I	Sigma	Cat# 9003-98-9
ACK lysing buffer	GIBCO	Cat#A1049201
Protein A agarose beads	Cell Signaling Technology	Cat#9863

SuperSignal West Pico Chemiluminescent Substrate	Thermo Fisher Scientific	Cat#34580
SuperSignal West Femto Maximum Sensitivity Substrate	Thermo Fisher Scientific	Cat#34095
RNAiso Plus	TaKaRa	Cat#9109
Seahorse XF^{e}24 FluxPax mini	Agilent	Cat#102342-100
Human TNF-α ELISA kit	Caymanchem	Cat#589201
PierceTM Agarose ChIP kit	Thermo Fisher Scientific	Cat#26156
BCA assay kit	Cell Signaling Technology	Cat#7780